# Development and Evaluation of Ultramicro Electrode Ensembles Based on 1.6-Hexanedithiol Self-Assembled Modified Layer and Its Application for HRP Detection

*Lixin Cao*[*]*, Qingchuan Li, Jiesheng Ji, Peisheng Yan, Tao Wang*

Department of Applied Chemistry, School of Ocean Science and Technology, Harbin Institute of Technology at Weihai, China
*E-mail: caolixin668@yahoo.com.cn

The 1.6-hexanedithiol (HDT) chemically modified gold (HDT/Au) electrode were prepared by self-assembly. The HDT modified layer blocked the heterogeneous electrolysis of $[Fe(CN)_6]^{3-/4-}$ strongly except sites of pinholes and defects which behaved like ultramicro electrode ensembles (UMEs). The features of UMEs and the electrochemcial characteristics of $[Fe(CN)_6]^{3-/4}$ at UMEs with different modifying hours were studied by electrochemical impedance spectroscopy. HDT modified gold electrode promoted the electrochemical process for redox reaction of 2,3-diaminophenazine (DAP), the product of OPD-$H_2O_2$-HRP enzymatic catalyst reaction system and blocked hydrogen evolution effectively. The detection limit determined by square wave was $10^{-11}$g/ml, which is about one order of magnitude lower than the reported lowest results.

## 1. INTRODUCTION

Self-assembled layers of thiols on gold have been the subject of considerable interest in the field of electroanalysis in recent years [1,2,3] due to their stability, high structure order, ease of preparation and flexibility in functional control by changing the endgroup. They have shown to be the promising materials to enable the interface to fulfill a variety of functions. Some densely packed thiol layers passivate electrode surfaces for some electroactive species and leave residual pinholes function effectively as gold ultra-microelectrode ensembles (UMEs) [4,5]. While some self-assembled layer modified electrodes can enhance both selectivity and sensitivity, improve the time response and decrease the overpotential [6,7]. Previous works have demonstrated the properties and applications strongly depend on their structures. A thiol molecule comprises three parts, the sulfur head group

forming a strong, covalent bond with gold substrate, the hydrocarbon chain stabilizing the SAM through van der Waals interactions, and the terminal group, which play particularly important roles in its functionality. A slight change in the end group might induce the remodeling of the physical and chemical properties of the modified layers [8,9,10]. The nature of modified layers with different endgroup have been studied broadly, ranging from hydrophobic groups, $-CH_3$, $-CH=CH_2$ to hydrophilic groups, $-COOH$, $-NH_2$, $-OH$ [11,12]. Even though a lot of work has been done for the understanding of the effect of terminal groups on the electrochemical responses of the redox species in solution [13,14,15], there are still many ambiguous and disputable factors needed to be clarified. Dithiols have $-SH$ as their terminal groups, which have been reported useful mainly in binding metallic ions and nanoparticles to the SAMs [16,17,18]. There also have been some reports on the structure features of dithiol layer on gold [19,20]. However, there has been very little research into characterizing $-SH$ terminal group as sensing interface so far.

Horseradish peroxidase (HRP) is the most commonly used enzyme label for enzyme linked immunoassay (ELISA) which is a very popular analytical method for samples of importance in clinical, pharmaceutical, environmental and food analysis [21,22,23]. HRP detection is performed as a crucial step of the assay for the determination of the targeted antibodies and antigens. Voltammetric Enzyme-linked Immunoassay has attracted intensive attention because of its short reaction time, excellent sensitivity and wide linear range, in which developing exquisite electrodes have been playing crucial roles [24,25,26].

In our present work, the 1.6-Hexanedithiol (HDT) chemically modified gold (HDT/Au) electrode were prepared and evaluated. The bare active gold surface formed by pinholes, collapsed sits and defects of self-assembed monolayers can be regarded as untramicro gold electrodes ensembles. We found 2,3-diaminophenazine (DAP), the product of O-phenylenediamine (OPD)-$H_2O_2$-HRP enzymatic catalyst system, have particular good electrochemical response at HDT/Au. The work on HDT/Au in the paper will not only be very helpful in determining its application for HRP based electrochemical enzyme immunoassay, but also provide meaningful information on the character of dithiol based sensing interfaces.

## 2. EXPERIMENTAL

### 2.1. Reagents and equipment

All chemicals used were of analytical grade and used as received without any further purification. The main reagents were 1.6-Hexanedithiol (Sigma Aldrich), Horseradish Peroxidase [RZ≥3.0, (unit, U)≥250U/mg, BBI]. Hydrogen peroxide (Shanghai)], O-phenylenediamine (Shanghai). O-phenylenediamine is a totoxic chemical and must be handled with care. All the solutions including the electrochemical studying solution with OPD and DAP were in brown container, because OPD and DAP were light sensitive. Double distilled water was used for rinsing and for all solutions.

Electrochemical impedance spectroscopy (EIS) was recorded using a Gamry PC4-750 (Germany) and cyclic voltammograms were recorded using Epsilon2000 electrochemical systems.

Conventional three-electrode systems were used in measurements, with a bare gold electrode, HDT/Au as the working electrodes, platinum as the counter and saturated calomel electrode (SCE) as the reference. For the ac impedance spectroscopy, the dc potential was set at zero overpotential and the ac potential was 5mV. The optimized SWV parameters for HRP detection were as follows: SWV amplitude: 25mV; step potential: 4mV; and frequency: 5Hz.

## 2.2. Preparation of 1.6-Hexanedithiol modified electrode by self-assembly

The working electrode which was polycrystalline gold disk of 3 mm in diameter was polished successively with wet alumina powder (0.3 and 0.05μm) to mirror-like, followed by cleaning in a piranha solution (1:3 mixture of 30% hydrogen peroxide and concentrated sulfuric acid) for 10 min, then rinsing with ethanol and water in an ultrasonic bath for 5 min, respectively. The polished electrode then was cleaned by voltammetrically cycling, between -0.1 and +1.2V vs SSE at a scan rate of 50mV/s in 0.5mol/L $H_2SO_4$ until a stable cyclic votammogram was obtained. Then, the electorde was immersed in ethanolic solution containing 10 mM HDT for the demanded hours. HDT/Au electrodes were rinsed with clean ethanol and successively with purified water.

## 3. RESULTS AND DISCUSSION

### 3.1. Characterizations of gold ultramicro ensembles based on 1.6-Hexanedithiol modification

The cyclic voltammgrams and Nyquist plots of [Fe $(CN)_6]^{3-/4-}$ at both bare gold and HDT/Au electrode with different modifying hours were shown in Fig. 1. As shown in Fig. 1(a), contrasted with the signal at bare gold electrode, the peak current values at HDT/Au electrodes reduced a lot, and the distances between the redox peak potential $\Delta E_p$ increased significantly with the increasing of modifying hours, and no obvious current peaks appeared after 3 hours. The longer the assembling hours, the higher density of HDT moleculars were rooted on gold surface. This indicates that the spots occupied by HDT moleculars blocked the heterogeneous electrolysis of $[Fe(CN)_6]^{3-/4-}$. The result was in consistent with reported thiols with hydrophobic $-CH_3$ [4,5] and hydrophilic group $-OH$, but was quite different from $-NH_2$ [12]. Literature [5,27,28] demonstrated that gold surface formed by pinholes, collapsed sits and defects of self-assembled monolayers can be regarded as untramicro gold electrode ensembles (UMEs), and HDT occupied area was inert. Fig. 2 shows the schematic diagram of HDT SAMs on the surface of Au. The fraction of active area and electrochemcial characteristics of $[Fe(CN)_6]^{3-/4}$ at UMEs with differne modifying hours were calculated from the results of Nyquist plots shown in Fig. 1(b)
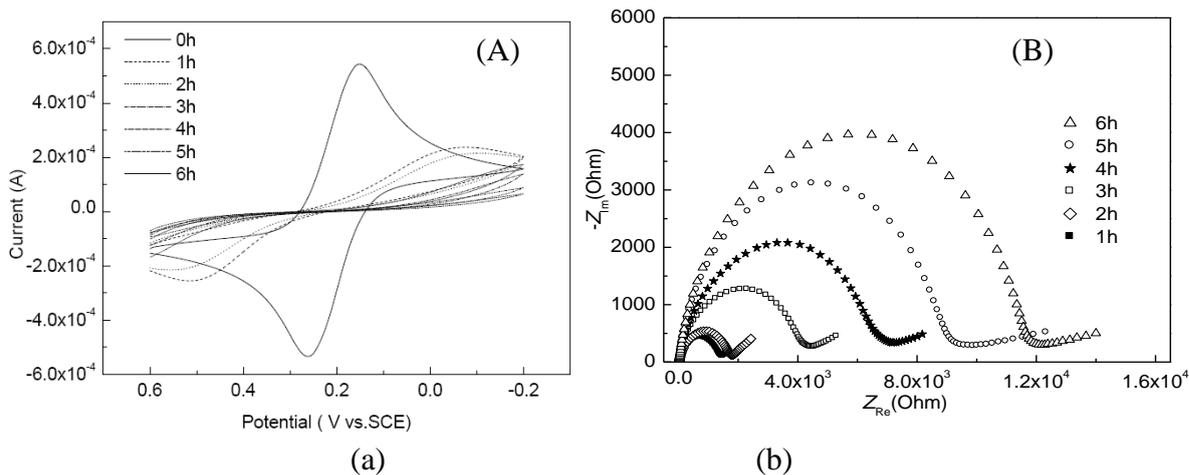
**Figure 1.** Cyclic voltammgrams (a ) and Nyquist plots (b) of 10 mM $K_3Fe(CN)_6$ + 10 mmol·$L^{-1}$ $K_4Fe(CN)_6$ + 1 mol/L KCl at bare gold and HDT/Au electrodes with different self-assembling hours. (the scan rate $v$=100 mV/s for CV; for Nyquist plots the frequencies ranging from 0. 01 ~100 k Hz )

At higher frequencies, within the domain where kinetic semicircles were observed, the redox reactions were totally controlled by the electron transfer kinetics. The semicircles increase with the longer self-assembling hours, indicating the charge transfer resistances of the electrochemical probe $[Fe(CN)_6]^{3-/4-}$ increased with the smaller active areas of gold UMEs.
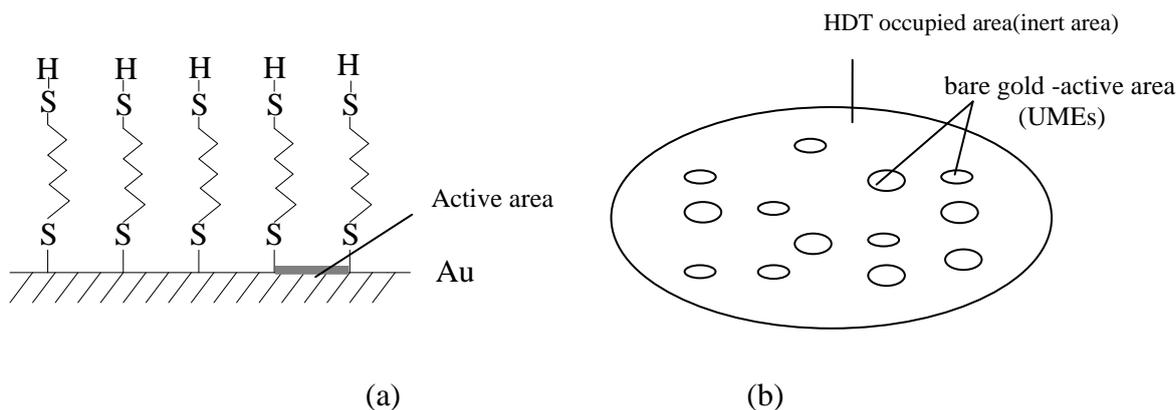


**Figure 2.** Schematic diagram of HDT SAMs on the surface of Au. (a) sulfur head group forming a strong, covalent bond with gold substrate. (b) regarded active areas of gold ultramicro ensembles (UMEs) formed by pinholes, collapsed sits and defects of self-assembed monolayers

This result was consistent with cyclic voltammetry results. At lower frequencies where the diffusion predominates, the slop of Warburg impedance was lesser than 0.5 which was only valid if the diffusion layer has an infinite thickness. Further more, the slop of Warburg impedance decrease steadily with the increase of HDT modifying hours. This could be ascribed to the fact that the areas of

gold ultramicro ensembles (UMEs) became smaller and the single elements of UMEs dispersed further away with the increase of self assembling hours. As a result, the adjacent spherical diffusion zones of the ultramicro patches overlapped lesser, the imaginary part dropped. These results were in agreement with that in literatures [29].

The total area fraction of UMEs and the electrochemcial characteristics of $[Fe(CN)_6]^{3-/4}$ at HDT/Au electrodes with differt self-assembling hours were shown in Table 1. According to literature [4,5] and our previous work [30], for a 1-electron, first-order reaction with $C_{ox}=C_{red}=C$ at ultramicro electrode ensembles (MHEEs), the following expressions were derived for real active area fraction calculation.

$$i_0 = \frac{RT}{R_{ct}nF} \tag{1}$$

$$i_0 = Fk_{app}C \tag{2}$$

$$k_{app}=k^o S_a/S_g \tag{3}$$

Where $i_0$ is the exchange current per unite geometric area, $k^o = 0.05$cm/s [27] and $k_{app}$ are the real and apparent rate constants; $S_a$ and $S_g$ are the active area of ultramicro ensembles (UMEs) and the geometric area of macro gold electrode, respectively. $S_a/S_g$ is the fraction of active area of ultramicro ensembles (UMEs), *R, T, n* and F has their usual meanings.

**Table 1**. Area fraction of Gold UMEs and electrochemcial characteristics of $[Fe(CN)_6]^{3-/4}$ at UMEs with differne modifying hours

| Self-assembling time | 1 h | 2 h | 3 h | 4 h | 5 h | 6 h |
|---|---|---|---|---|---|---|
| $R_{ct}(\Omega)$ | 1377 | 1712 | 4137 | 6587 | 8690 | 11199 |
| $i_0$ | $1.9\times10^{-5}$ | $1.5\times10^{-5}$ | $6.2\times10^{-6}$ | $3.9\times10^{-6}$ | $3.0\times10^{-6}$ | $2.3\times10^{-6}$ |
| $k_{app}$ | $2.8\times10^{-4}$ | $2.2\times10^{-4}$ | $9.0\times10^{-5}$ | $6.0\times10^{-5}$ | $4.4\times10^{-5}$ | $3.4\times10^{-5}$ |
| $S_a/S_g$ | $5.5\times10^{-3}$ | $4.4\times10^{-3}$ | $1.8\times10^{-3}$ | $1.2\times10^{-3}$ | $8.7\times10^{-4}$ | $6.8\times10^{-4}$ |
| Slops of Warburg impedance | 0.48 | 0.46 | 0.23 | 0.16 | 0.11 | 0.10 |

The software ZSimpWin was employed for simulation of the EIS response, and the equivalent circuit was $R(Q(R_{ct}W)$. It should be noted that there were some differences in the quantity results between electrodes with different surface condithion, because the arrangement of self-assembled layer strongly rely on the substrate [6]. However the trends were simillar. The purpose of the quantity results in this work was to elucidate the trend and evaluation method.

*3.2. Charcteristics of OPD-H₂O₂-HRP enzymatic system at HDT/Au electrodes*

*3.2.1 The opitimazaiton of OPD-H₂O₂-HRP enzymatic catalyst reaction system*

       The result cyclic voltammograms of The HDT/Au electrode with different modification hours showed the fact that 2 h modification performanced well in terms of the redox current value and hydrogen evolution.

       The cyclic voltammetry was employed for the optimization of the OPD-$H_2O_2$-HRP enzymatic catalyst reaction system. The optimized concentration of OPD and $H_2O_2$ were $7.4 \times 10^{-3}$ mol/L and $4.0 \times 10^{-4}$ mol/L. Buffer solution were 0.05 mol/L di-sodium hydrogen phosphate-citrate solution with 5.0 pH value, temperature 30℃. Enzymatic catalyst reaction time was 60 min. The samples were prepared and detected by an interval of 15 min to ensure the same time for enzymatic catalyst reaction. Our experimental results demonstrated that this method was more precise and time saving than that using the commonly used process: ending enzymatic catalyst reaction by acid and then neutralizing and adjusting to proper pH values.

*3.2.4 Electrochemical characteristics of DAP at HDT/Au electrode*

       Figure 3 showed the result of cyclic voltammetry of DAP at bare gold and HDT/Au electrode with two hours modification. The concentration of HRP was $2 \times 10^{-9}$ g/mL. Other components and parameters such as pH value, incubation temperature and reaction time were as the optimized.

       There were cathodic and anodic current peaks at both Au and HDT/Au electrode due to reduction and oxidization of 2, 3-diaminophenazine [31]. However, compared to the behavior observed at bare gold electrode, the cathodic peak at HDT/Au electrode shifted to more positive potentials. The base current was decreased remarkably by the HDT modification, and the DAP voltametric response was much better resolved.
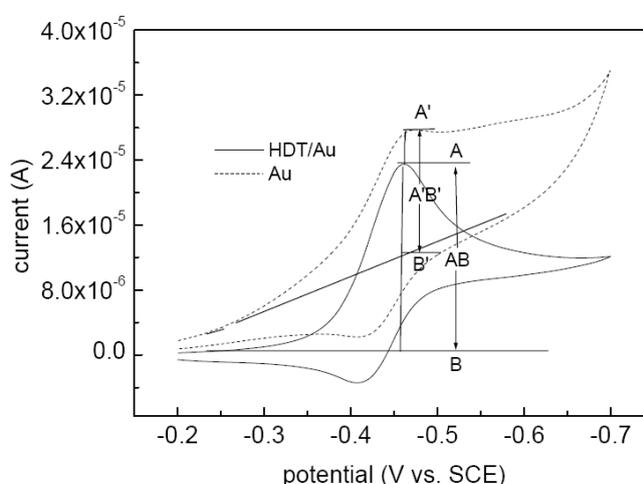


**Figure 3.** Cyclic voltammograms of DAP at gold and HDT/Au electrodes with two hours self-assembling, v= 50mv/s

The cathodic peak current value AB at HDT/Au electrode was $2.300 \times 10^{-5}$A, 1.6 times higher than that at Au electrode (A'B' $=1.443 \times 10^{-5}$ A). In addition, at bare gold electrode, the current increased obviously when the potentials were minus than -0.57V, owing to hydrogen evolution. However, hydrogen evolution did not appear until the potential reached -0.70V at HDT/Au electrode, indicating that HDT layer blocked hydrogen evolution effectively.

These differences demonstrated the fact that the SAM has the ability to prevent the adsorption of HRP and give a well-defined CV forfile. These differences showed the fact that the HDT SAM does not work as the barrier for organic molecules, unlike for inorganic $[Fe(CN)6]^{3-/4-}$ redox couple, but a well-defined CV forfile. These might be ascribed to the fact that the HDT modified layer has the ability to prevent the adsorption of HRP [32] and promoted the electrochemical process of DAP. Considering the structure of –SH and DAP, the improvement might be owing to p-p conjugative effect between the lone electron pair of S atom and the nitrogen atom in 5,10-imino groups, p-π between S atom and the aromatic ring of DAP. The interaction schematic diagram of HDT with DAP molecule were shown in Fig. 4.
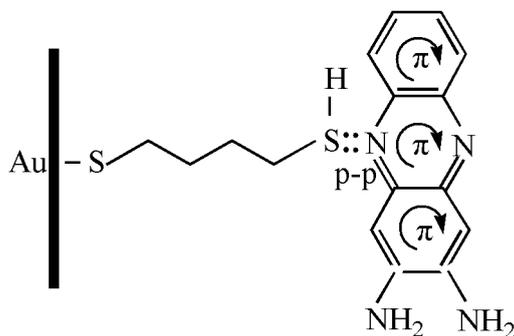


**Figure 4.** Schematic diagram of the interactions between the HDT layer and DAP molecular
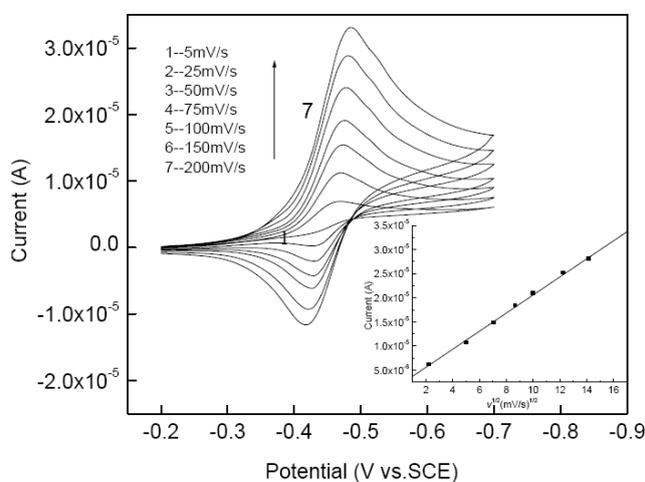


**Figure 5.** Cyclic voltammograms of DAP at HDT/Au electrode with two hours self-assembling at scan rates from 5mV/s to 200mV/s, the inserted was the corresponding plots of the reduction peak currents $I_{pc}$ versus scan rates $v$

The cyclic voltammograms of DAP at HDT/Au electrode with 2 h modifying hours at scan rates from 5mV/s to 200mV/s were shown in Fig. 5. The inserted was the corresponding plots of the reduction peak currents $I_{pc}$ versus scan rates $v$. $I_{pc}$ was found to display a linear dependence on $v^{1/2}$ (correlation coefficient $r = 0.9989$) , indicating that the reduction process of DAP at HDT/Au electrode was controlled by reactant diffusion. The slightly increase of peak separation with scan rate indicates that the process is a quasi reversible redox process. More details on electrochemical kinetic of DAP at HDT/Au electrode will be further investigated by pure DAP.

### 3.3. Determination of the concentration of HRP in enzymatic catalystic system

The square wave voltammetry was employed to determine the concentration of HRP. Fig. 6 displayed the SW voltammograms for HRP enzyme catalytic system with different concentration of HRP and calibration curve versus concentration. The cathodic peak current increased with the increase of HRP concentration and exhibited a linear relation from $2\times10^{-11}$ to $1\times10^{-9}$ M (correlation coefficient, r = 0.9935). The detection limit was as low as $1\times10^{-11}$ M (S/N=3), almost one order of magnitude lower than the reported lowest results at GC electrode [33]. The relative standard deviation for twelve parallel determinations with $1\times10^{-10}$ was 3.2%. The stability might be ascribed to the function of −SH end group.
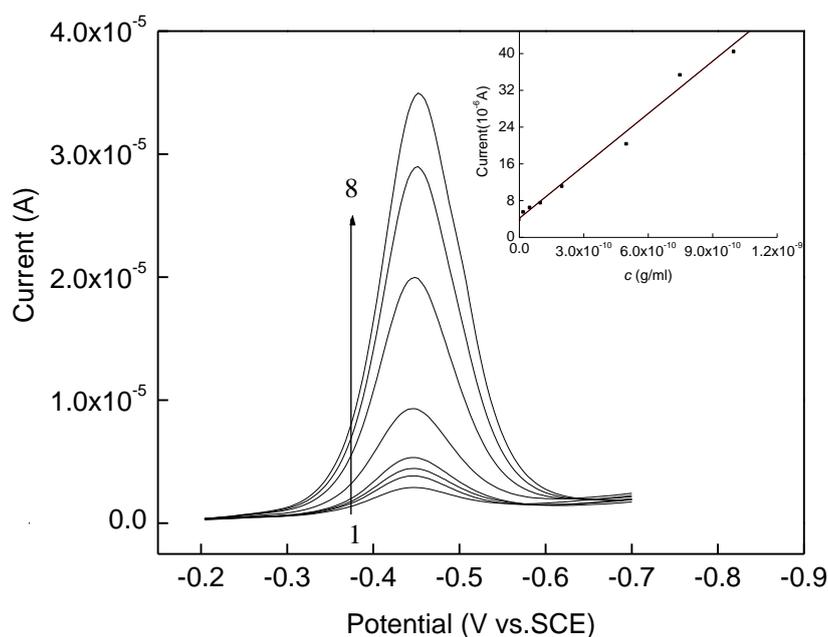


**Figure 6.** SW voltammograms of HRP enzyme catalytic system with different concentration of HRP at HDT/Au electrode with two hours self-assembling (1: 0；2: $2\times10^{-11}$; 3: $5\times10^{-11}$; 4: $1\times10^{-10}$; 5: $2\times10^{-10}$; 6: $5\times10^{-10}$; 7: $7.5\times10^{-10}$; 8: $1\times10^{-9}$g/mL ), the inserted is corresponding current vs. concentrations

## 4. CONCLUSIONS

The HDT monolayer showed the different performance between inorganic redox couple $[Fe(CN)_6]^{3-/4-}$ and organic substance DAP. For $[Fe(CN)_6]^{3-/4-}$, the active areas were the UEMs, which were composed by pinholes, defects and collapsed sits of HDT monolayer blocking the electroanalysis of $[Fe(CN)_6]^{3-/4-}$. However the HDT modified gold electrode promoted electrochemical process of DAP, giving a well-defined CV profile, and reached lowered HRP detection limit. The unexpected beneficial performance of HDT/Au electrode might be mainly ascribed to the interaction between the end group −SH of HDT and DAP molecules. The pathway for electron transfer between the electrode surface and DAP was by electron tunneling through the HDT film. Besides, the HDT layer was helpful for preventing HRP preferentially adsorbed to bare gold surface.

The results from this work show the promise for dithiol modified electrode based electrochemical biosensors targeted for HRP labeled voltammetric Enzyme-linked Immunoassay. In addition, this research provides a meaningful clue for the study and application of dithiol as sensing interface.

## References

1. J. J. Gooding, and D. B. Hibbert, *Trends Anal. Chem.*, 18 (2009) 525
2. A. M. Luque, W. H.Mulder, and J. Jose Calvente, *Analytical Chemistry*, 84 (2012) 13
3. L. Jia, X. H. Zhang, Q. Li, and S. F. Wang, *J. Anal. Chem.*, 62 (2007) 266
4. E. Sabatani, and I. Rubinstein, *J. Electroanal Chem.*, 219 (1987) 365
5. H. Finklea, D.A. Snider, and J. Fedyk, *Langmuir.*, 9 (1993) 3660,
6. M. B. Moressi, R. Andreu, and J. J. Calvente, *J. Electroanal. Chem.,* 570 (2004) 209,
7. J. J. Gooding, F. Mearns, W. Yang, and J. Liu, *Electroanal.* 15 (2003) 81,
8. G. Heimel. F. Rissner, and E. Zojer, *Adv. Mater.*, 22 (2010) 2494
9. P. L. Schilardi, P. Dip, P. C. dos Santos Claro, G. A. Benítez, M. H. Fonticelli, O. Azzaroni, and R. C. Salvarezza, *Chem.-Eur.,* 12 (2006) 38
10. D. Burshtain, and D. Mandler, *Phys. Chem. Chem. Phys.*, 8 (2006) 158
11. L. X. Cao, P. S. Yan, K. N. Sun, and W. D. Kirk, *Electrochim. Acta*, 53 (2008) 8144
12. K. Takehara, H. Takemura, and Y. Ide, *Electrochim. Acta,* 39 (1994) 817,
13. K.Takenhara, and H. Takemura, *Bull Chem. Soc. Jpn*. 68 (1995) 1289
14. R. J. Janek, and W. R. Fawcett, *Langmuir*, 14 (1998) 3011
15. C. E. D. Chidsey, *Science*, 251 (1991) 919
16. J. Li, Z. H. Wu, and G. Wang, *Sens. Actuators, B*, 110 (2005) 327
17. F. Schreiber, *Prog. Surf. Sci.*, 65 (2000) 151
18. F. Arduini, C. Majorani, and A. Amine, *Electrochimica Acta,* 56 (2011) 4209.
19. M. J. Esplandiu, P.-L. And M Moeske, *Appl. Surf. Sci.*, 199 (2002) 166
20. M. Silvestrini, P. Schiavuta, P. Scopece, G. Pecchielan, L. M. Morretto, and P. Ugo, *Electrochimica Acta*, 56 (2011)7718

21. S. Suresh, A. K. Gupta, V. K. Rao, O. Kumar, and R. Vijayaraghavan, *Talanta*, 81(2010) 703
22. N. Laboria, A. Fragoso, W. Kemmner, D. Latta, O. Nilsson, M. L. Botero, K. Drese, and C. K. O'Sullivan, *Anal. Chem.*, 82(2010) 1712
23. S. Piermarini, L. Micheli, N. H. Ammida, G. Palleschi, D. Moscone, *Biosens Bioelectron.*, 22 ( 2007) 1434
24. J. S. Rossier, H. and H. Girault, *Lab on A Chip*, 1 (2001) 153
25. Z. Dai, J. Chen, F. Yan, and H. X. Ju, *Cancer Detection and Prevention*, 29 (2005) 233
26. J. P. Li, H. L. Gao, Z. Q. Chen, X. P. Wei, and C. F. Yang, *Analytica Chimica Acta*, 665 (2010) 98
27. E. Sabatani, and I. Rubinstein, *J. Phys. Chem.*, 91 (1987) 6663
28. P. Diao, M.Guo, and R. Tong, *J. Electroanal. Chem.*, 495 (2001)98
29. C. N. Cao, and J. Q. Zhang. *Introduction to Electrochemical impedance spectroscopy.* Science Press, Beijing (2002)
30. L. X. Cao, P. S. Yan, K. N. Sun, and W. D. Kirk, *Electroanalysis*, 21 (2009) 1183
31. W. Sun, K. Jiao, and S. S Zhang, *Talanta*, 55 (2001)1211
32. K. Takehara, H. Takemura, and Y. de, *J. Colloid Interface Sci.*, 156 (1993)274
33. K. Jiao, W. Sun, H. and Y. Wang, *J. Anal. Sci.*, 20 (2004) 341